Chinese Journal of Catalysis 36 (2015) 299–307

available at www.sciencedirect.com

ScienceDirect

journal homepage: www.elsevier.com/locate/chnjc

Article

Preyssler heteropolyacid supported on silica coated $NiFe_2O_4$ nanoparticles for the catalytic synthesis of bis(dihydropyrimidinone)benzene and 3,4-dihydropyrimidin-2(1*H*)-ones

Hossein Eshghi [a], Ali Javid [b,*], Amir Khojastehnezhad [a,#], Farid Moeinpour [c], Fatemeh F. Bamoharram [d], Mehdi Bakavoli [a], Masoud Mirzaei [a]

[a] *Department of Chemistry, Faculty of Sciences, Ferdowsi University of Mashhad, Mashhad, Iran*
[b] *Department of Chemistry, Ahvaz Branch, Islamic Azad University, Ahvaz, Iran*
[c] *Department of Chemistry, Bandar Abbas Branch, Islamic Azad University, Bandar Abbas, 7915893144, Iran*
[d] *Department of Chemistry, College of Science, Mashhad Branch, Islamic Azad University, Mashhad, Iran*

ARTICLE INFO

Article history:
Received 19 October 2014
Accepted 12 December 2014
Published 20 March 2015

Keywords:
Preyssler
Nickel ferrite nanoparticles
Magnetically green catalyst
Bis(dihydropyrimidinone)benzene
3,4-Dihydropyrimidin-2(1*H*)-ones

ABSTRACT

A novel magnetic acidic catalyst comprising Preyssler ($H_{14}[NaP_5W_{30}O_{110}]$) heteropoly acid supported on silica coated nickel ferrite nanoparticles ($NiFe_2O_4@SiO_2$) was prepared. The catalyst was characterized by Fourier transform infrared, scanning electron microscopy, transmission electron microscopy, X-ray diffraction, energy dispersive spectrum, VSM and particle size neasurement. Its catalytic activity was investigated for the synthesis of bis(dihydropyrimidinone)benzene and 3,4-dihydropyrimidin-2(1*H*)-ones derivatives by the Biginelli reaction. With the catalyst, the reactions occurred in less than 1 h with good to excellent yields. More importantly, the catalyst was easily separated from the reaction mixture by an external magnet and reused at least five times without degradation in the activity.

1. Introduction

In recent decades, magnetic nanoparticles (MNPs) have been widely studied for various biological and medical applications [1,2]. They have been shown to be promising supports for the immobilization of catalysts because magnetic catalysts can be easily separated from the reaction medium by an external magnet, which provides a simple separation of the catalyst without the need for filtration, centrifugation, or other tedious workup processes [3]. This separation technique has a special importance for nano-sized catalyst supports where filtration methods result in the loss of catalyst particles and product contamination. Apart from an easy separation, an interesting property of MNPs is that an appropriate surface modification provides a wide range of magnetic-functionalized catalysts that show equal and sometimes higher activity than their homogeneous catalysts in organic transformations. In recent years, MNPs as catalyst or catalyst support have been widely used in a variety of important organic reactions including C-C coupling [4–6], reduction [7–9], oxidation [10–15] and multicomponent reactions [16–19] with high activity.

Recently, Wang et al. [20] reported the synthesis of silica

---

* Corresponding author. Tel: +98-511-8435000; Fax: +98-511-8435115; E-mail: alijavids@yahoo.com
\# Corresponding author. Tel: +98-511-8435000; Fax: +98-511-8435115; E-mail: akhojastehnezhad@yahoo.com

DOI: 10.1016/S1872-2067(14)60265-5 | http://www.sciencedirect.com/science/journal/18722067 | Chin. J. Catal., Vol. 36, No. 3, March 2015

coated Fe_3O_4 MNPs for immobilizing heteropoly acids (HPAs) with a Keggin structure (tungstophosphoric acid). Their synthesized catalyst was a magnetically separable catalyst and after completion of the reaction, it was easily separated by an external magnet. Rafiee et al. [21–23] reported another silica coated MNPs with the formula $Fe_2O_3@SiO_2$ for supporting tungstophosphoric acid and phosphomolybdic acid. They showed good catalytic activity by these catalysts. In addition to Fe_3O_4 and Fe_2O_3, there are other iron oxides with the ferrite structure and general formula (AFe_2O_4), where A can be Mn, Co, Ni, Cu, and Zn [24–26]. Ni ferrites ($NiFe_2O_4$) are one of the most versatile magnetic materials with a high saturation magnetization, high Curie temperature, chemical stability, and relatively high permeability [27], and because of these magnetic properties it can be used as a magnetic source.

The Preyssler HPA ($H_{14}NaP_5W_{30}O_{120}$) is a HPA which has significant advantages, such as 14 acidic protons, high thermal stability, high hydrolytic stability ($0 < pH < 12$), regenerability and safety [28,29]. Owing to the low surface area (7–10 m^2/g) and high solubility of HPAs in polar solvents, it is preferrable to use them in supported form. These catalysts can be supported on neutral solids, such as silica, activated carbons, or zeolites and acidic ion exchange resins [29,30]. Recently, we supported Preyssler HPA on silica and used this supported catalyst for various reactions [29,31–33]. Several advantages of using supported HPAs compared to the homogeneous catalyst include easier recovery and recycling after reaction and easier product separation [34]. However, the separation and recovery of the immobilized Preyssler on silica is usually performed by filtration or centrifugation, which are not eco-friendly processes. The immobilization of this HPA on silica-coated MNPs with a new structure ($NiFe_2O_4$) can be employed to develop a novel heterogeneous catalyst system which is magnetic that possesses both a high separation efficiency and a relatively high surface area to maximize catalyst loading and activity.

In a continuation of our achievements in the preparation of novel catalysts [35–38] and based on our previous success in the preparation of MNPs as catalysts [39–41], in this study, we supported Preyssler HPA on $NiFe_2O_4@SiO_2$ (denoted NFS-PRS). After the characterization of this novel magnetically recoverable catalyst, its catalytic activity was tested in the synthesis of bis(dihydropyrimidinone)benzene and 3,4-dihydropyrimidin-2(1*H*)-ones and -thiones derivatives by the Biginelli reaction. The synthesis of these products occurred from the condensation of terephthalic aldehyde, urea and 1,3-dicarbonyl compound. This is a simple, green, and efficient synthesis method with these reactions using NFS-PRS as a heterogeneous and highly active acidic catalyst (Scheme 1).

2. Experimental

All reagents were purchased from Merck and Aldrich and used without further purification. Melting points were determined on an Electrothermal Type 9100 melting point apparatus. The particle size and morphology of the synthesized catalyst were characterized with a transmission electron microscope (TEM, Philips CM-200 and Titan Krios) and scanning electron microscope (SEM, Philips XL 30 and S-4160) with a gold coating. X-ray diffraction (XRD) measurements were performed using a Bruker AXS Company, D8 ADVANCE diffractometer (Germany). Infrared (IR) spectra were recorded on a Thermo Nicolet AVATAR-370 FT-IR spectrophotometer and ^1H NMR spectra were recorded on a Bruker DRX400 spectrometer.

2.1. *Preparation of NFS-PRS*

The core-shell silica nickel ferrite (NFS, Fig. 1) was synthesized according to our previous reports [39–41]. Afterwards, for the immobilization of Preyssler HPA on the NFS, 0.75 g of Preyssler was dissolved in 5 mL of water. This solution was added dropwise to a suspension of 1.0 g of NFS in water (50 mL). The mixture was stirred for 12 h at room temperature under vacuum. After stirring for the specified time, the solvent was evaporated off and the supported catalyst collected by a permanent magnet and dried in a vacuum overnight. After the

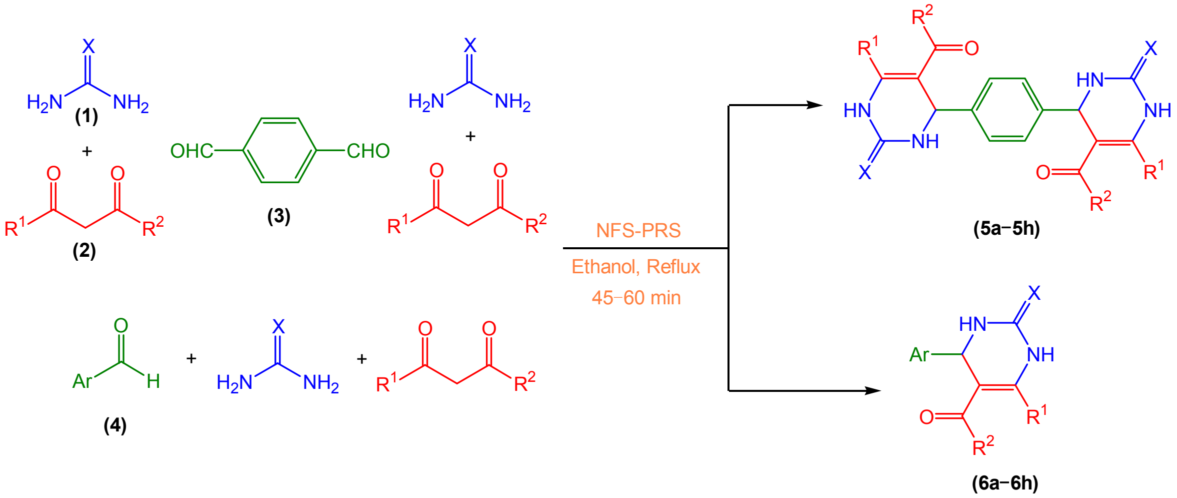

Scheme 1. Synthesis of bis(dihydropyrimidinone)benzene and 3,4-dihydropyrimidin-2(1*H*)-ones and -thiones derivatives using NFS-PRS as a nano magnetic catalyst.

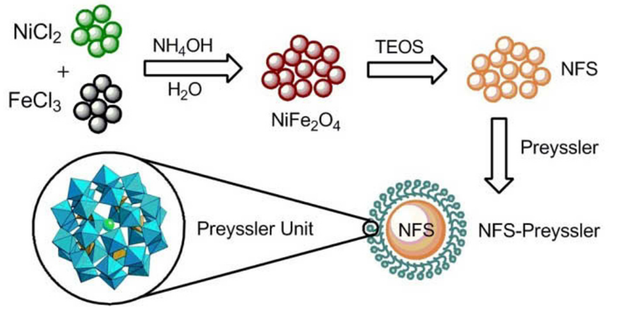

Fig. 1. Preparation of NFS-PRS.

drying, the supported nano catalyst was calcined at 250 °C for 2 h [31].

2.2. *Synthesis of bis(dihydropyrimidinone)benzene derivatives (**5a**–**5h**)*

The NFS-PRS catalyst (0.02 g) was added to a solution of terephthalic aldehyde (1.0 mmol), urea (2.5 mmol) and 1,3-dicarbonyl compound (2.0 mmol) in ethanol (10 mL) and refluxed for 45–60 min. Upon completion, the reaction mixture was allowed to cool to room temperature and the NFS-PRS was separated from the reaction mixture by an external magnet and thoroughly washed and dried to be reused in the next run. Cold water (20 mL) was added to the reaction mixture (without a catalyst) and after stirring for a few minutes, the solid product formed was filtered off and washed several times with cold ethanol and water. The resulting crude product was recrystallized from ethanol and gave compounds **5a**–**5h** in high yields.

2.3. *Selected spectroscopic data*

Diethyl-4,4'-(1,4-phenylene)bis(6-methyl-2-oxo-1,2,3,4-tetrahydropyrimidine-5-carboxylate) (**5b**). ^{1}H NMR(400 MHz, DMSO-d$_6$): δ 1.0 (6H, t, J = 7.2 Hz, OCH$_2$CH$_3$), 2.23 (6H, s, CH$_3$), 3.9 (4H, q, J = 7.3 Hz, OCH$_2$CH$_3$), 5.1 (2H, d, J = 3.2 Hz, CH), 7.17 (4H, s, Ph), 7.69 (2H, s, NH), 9.17 (2H, d, J = 1.6 Hz, NH); IR (KBr, cm^{-1}): υ 3365, 3239, 3104, 2971, 1701, 1647, 1459, 1223, 1084; MS (m/z): 442 (M$^+$), 255, 236, 149, 124, 97, 83, 69, 57; Anal. Calcd.: C, 59.72; H, 5.92; N, 12.66. Found: C, 59.58; H, 5.94; N, 12.71.

4,4'-(1,4-phenylene)bis(5-acetyl-6-methyl-3,4-dihydropyrimidin-2(1*H*)-one) (**5c**). ^{1}H NMR (400 MHz, DMSO-d$_6$): δ 2.07 (6H, s, CH$_3$), 2.37 (6H, s, COCH$_3$), 5.1 (2H, d, J = 3.6 Hz, CH), 7.18 (4H, s, Ph), 7.71 (2H, s, NH), 9.1 (2H, d, J = 1.6 Hz, NH); IR (KBr, cm^{-1}): υ 3423, 3284, 1686, 1655, 1610, 1577, 1184, 1109, 1018; MS (m/z): 382 (M$^+$), 369, 301, 236, 97, 83, 69, 57.

4,4'-(1,4-phenylene)bis(5-benzoyl-6-methyl-3,4-dihydropyrimidin-2(1*H*)-one) (**5d**). ^{1}H NMR (400 MHz, DMSO-d$_6$): δ 1.65 (6H, s, CH$_3$), 5.20 (2H, d, J = 3.2 Hz, CH), 7.13 (4H, s, Ph), 7.3–7.5 (10H, m, COPh), 7.76 (2H, s, NH), 9.15 (2H, s, NH); IR (KBr, cm^{-1}): υ 3400, 3096, 1685, 1417, 1179.

4,4'-(1,4-phenylene)bis(5-acetyl-6-(trifluoromethyl)-3,4-dihydropyrimidin-2(1*H*)-one) (**5e**). ^{1}H NMR (400 MHz, DMSO-d$_6$): δ 2.03 (6H, s, CH$_3$), 5.14 (2H, d, CH), 7.31 (4H, s, Ph), 7.76 (2H, s, NH), 9.48 (2H, s, NH); IR (KBr, cm^{-1}): υ 3412, 3101, 1680, 1415, 1159.

2.4. *Synthesis of 3,4-dihydropyrimidin-2(1H)-ones and -thiones derivatives (**6a**–**6h**)*

Similar to the above synthesis method, NFS-PRS catalyst (0.02 g) was added to a solution of aromatic aldehyde (1.0 mmol), urea (1.2 mmol) and 1,3-dicarbonyl compound (1.0 mmol) in ethanol (10 mL) and refluxed for 15–30 min. Upon completion, the reaction mixture was allowed to cool to room temperature and the NFS-PRS was separated from the reaction mixture by an external magnetic field and thoroughly washed and dried to be reused in the next run. Cold water (40 mL) was added to reaction mixture (without a catalyst) and after stirring for a few minutes, the solid product formed was filtered off and washed several times with cold ethanol and water. The resulting crude product was recrystallized from ethyl acetate/ *n*-hexane and gave compounds (**6a**–**6h**) in high yields.

3. Result and discussion

3.1. *Characterization of NFS-PRS*

The NFS-PRS catalyst was prepared by the route outlined in Fig. 1. Magnetic NiFe$_2$O$_4$ nanoparticles were prepared by the chemical method and subsequently were coated with tetraethyl orthosilicate to get silica coated nickel ferrite nanoparticles (NFS). Finally, the Preyssler HPA was supported on the silica coated MNPs to give the corresponding Preyssler HPA supported on the magnetic nanoparticles (NFS-PRS). The catalyst was characterized by FT-IR, TEM and particle size analysis, SEM and EDS, XRD and VSM.

The FT-IR spectra of NFS, Preyssler and NFS-PRS are shown in Fig. 2. NFS exhibited highly intense absorption peaks at 1200 and 1100 cm^{-1}. These peaks are assigned to the longitudinal and transverse stretching vibration modes of the Si–O–Si asymmetric bond. Additional bands at 812 and 470 cm^{-1} were identified as the characteristic peaks of the Si–O–Si bond. The other peak observed at 950 cm^{-1} assigned to the SiO$_3^{2-}$ vibra-

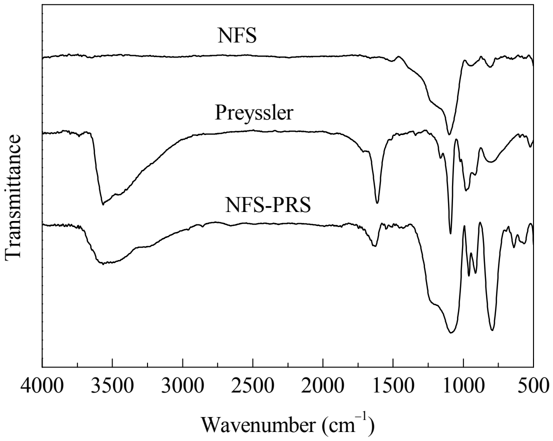

Fig. 2. FT-IR spectra of NFS, Preyssler HPA, and NFS-PRS.

tions indicated the existence of nonbridging oxygen ions [29,31]. Preyssler HPA displayed vibrations at 1162, 1090, and 1025 cm^{-1} for the P–O stretching in the Preyssler structure, 980 and 906 cm^{-1} for W–O–W stretching, 802 cm^{-1} for W=O stretching, and 522 cm^{-1} for P–O bending [42]. There was also a highly intense absorption peak at 1630 cm^{-1}, which was attributed to adsorbed water [20]. In the NFS-PRS, the peaks in the regions of 3563, 1090, 960, 913, 794, and 566 cm^{-1} confirmed the successful immobilizing of the Preyssler HPA on the surface of the silica coated nickel ferrite NPs.

Fig. 3 shows TEM images of the synthesized NFS and NFS-PRS MNPs. In the NFS-PRS, the darker parts proved good immobilizing of Preyssler HPA on the NFS. Also, the particle size distribution (Fig. 3(c)) of the NFS NPs showed that these MNPs have a size between 25 to 97 nm and a mean diameter of 53 nm. The morphological features were examined by SEM. The SEM images before (Fig. 4(a)) and after (Fig. 4(b)) supporting Preyssler HPA on the NFS demonstrated that these MNPs were almost spherical and regular in shape. However, aggregation of the nanoparticles was found. This aggregation may have occurred during the coating and supporting process. In the energy dispersive spectrum (EDS) of NFS-PRS (Fig. 4(c)), the tungsten peaks confirmed the successful immobilizing of the Preyssler HPA on the surface of the silica coated nickel ferrite MNPs. These observations were in agreement with the FT-IR results.

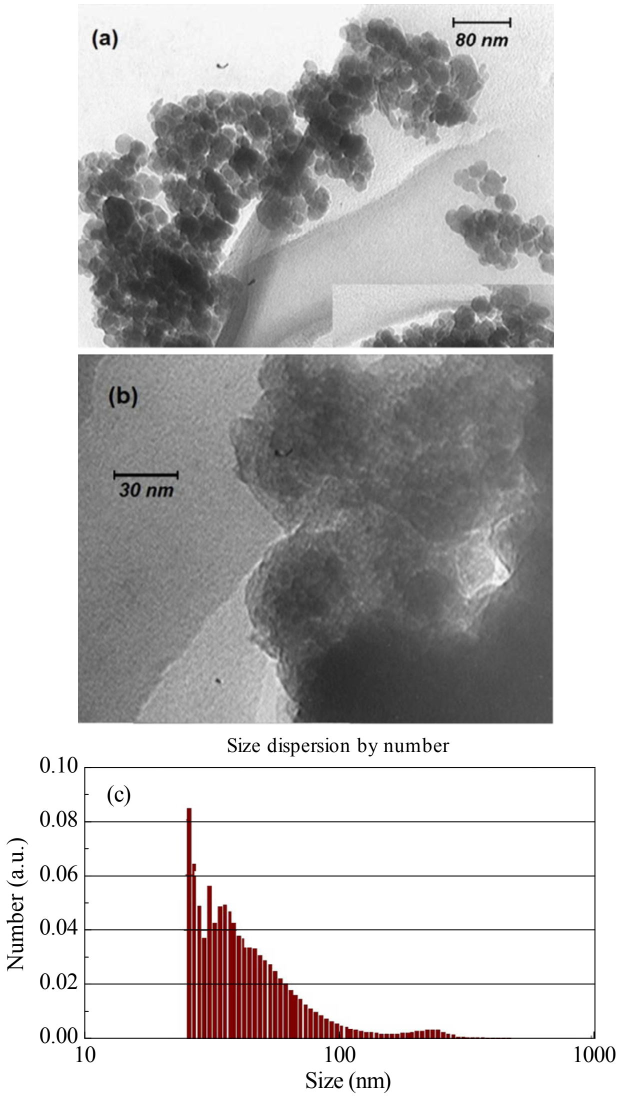

Fig. 3. TEM images of NFS (a) and NFS-PRS (b) and particle size distribution of NFS (c).

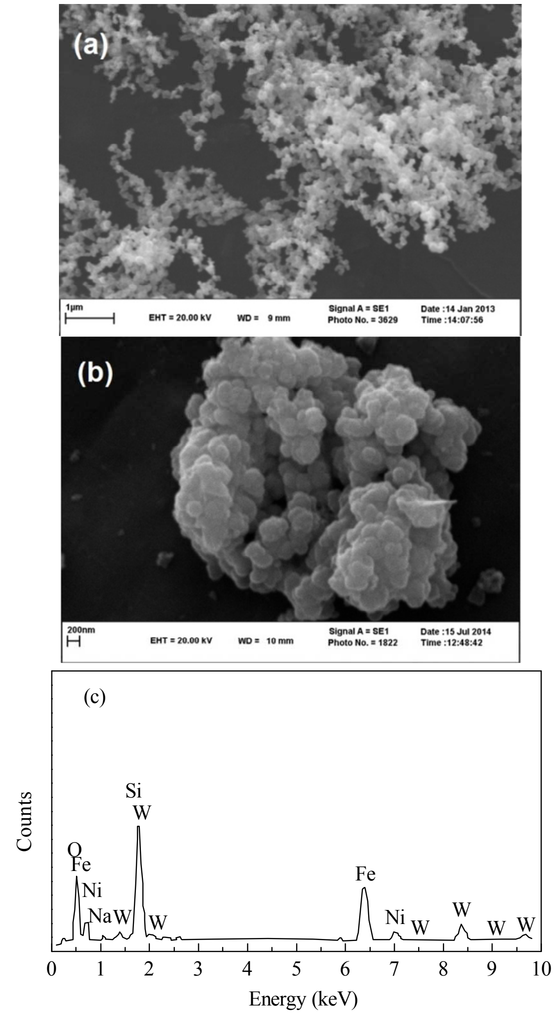

Fig. 4. SEM images of NFS (a) and NFS-PRS (b) and EDS spectrum of NFS-PRS (c).

In our previous work [40], we supported HPAs with Keggin structures on silica coated $NiFe_2O_4$. The structure of these MNPs before and after the supporting were compared using XRD analysis. We showed that there was no separate crystal phase that was characteristic of a Keggin HPA in the supported form. The broad peak at 2θ = 20°–30° that appeared was related to the amorphous silica phase in the shell of $NiFe_2O_4$ [43]. In the XRD pattern of NFS-PRS (Fig. 5), the characteristic peaks at 2θ = 30°, 35°, 43°, 54° 57, and 63° were similar to the previously reported data for $NiFe_2O_4$ MNPs [44,45], and the broad peak at 2θ = 20°–30° can be assigned to an amorphous silica phase in the shell of $NiFe_2O_4$. Similar to our previous work, there was no characteristic peak of the Preyssler HPA in the XRD pattern [20]. These observations indicated that the Preyssler HPA was well dispersed on the surface of the silica coated MNPs since there was no crystalline phase of this HPA

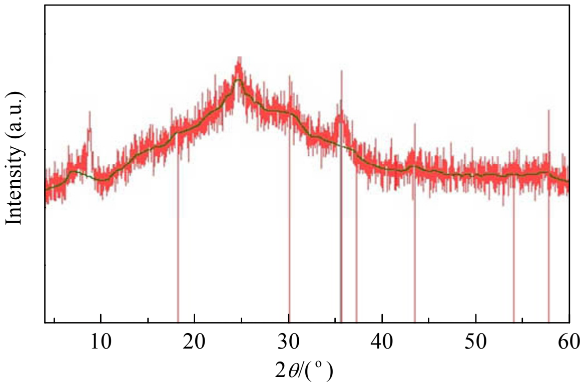

Fig. 5. XRD pattern of NFS-PRS.

Table 1
Comparison of different solvents and catalysts for the synthesis of bis(dihydropyrimidinone)benzene derivatives (**5b**).

Entry	Catalyst	Solvent	Time (min)	Temperature (°C)	Isolated yield (%)
1	None	C_2H_5OH	120	78	no reaction
2	NFS-PRS	solvent-free	120	80	34
3	NFS-PRS	H_2O	60	100	no reaction
4	NFS-PRS	$CH_3CO_2C_2H_5$	60	77	trace
5	NFS-PRS	CH_3CN	60	82	36
6	NFS-PRS	CH_3CO_2H	60	118	85
7	NFS-PRS	C_2H_5OH	45	78	92
8	NFS-PRS	C_2H_5OH	90	78	93
8	SiO_2-PRS	C_2H_5OH	45	78	85
9	Preyssler	C_2H_5OH	45	78	84
10	$H_4[SiW_{12}O_{40}]$	C_2H_5OH	60	78	49
11	$H_3[PW_{12}O_{40}]$	C_2H_5OH	60	78	61
12	$H_3[PMo_{12}O_{40}]$	C_2H_5OH	60	78	40

Reaction conditions: Terephthalic aldehyde **1** (1.0 mmol), urea **2** (2.5 mmol) and ethyl acetoacetate **3** (2.0 mmol).

detected by XRD analysis.

It is important that the core/shell material possess sufficient magnetic and superparamagnetic properties for practical applications. Magnetic hysteresis measurements for the $NiFe_2O_4$ were done in an applied magnetic field at room temperature with the field swept from −10000 to +10000 Oe. As shown in Fig. 6, the M (H) hysteresis loop for the samples was reversible, showing that the nanoparticles exhibit superparamagnetic characteristics. The hysteresis loops of these reached saturation at the maximum applied magnetic field. The magnetic saturation value of $NiFe_2O_4$ was 16.71 emu/g at room temperature. These MNPs showed high permeability in magnetization and their magnetization was sufficient for easy magnetic separation with a normal magnet.

3.2. *Evaluation of the catalytic activity of NFS-PRS*

Initially, in order to optimize the reaction conditions, the synthesis of compound **5b** was used as a model reaction. A mixture of terephthalic aldehyde (1.0 mmol), urea (2.5 mmol) and ethyl acetoacetate (2.0 mmol) in the presence of NFS-PRS was heated in different solvents and under a solvent-free condition to assess the effect of the solvent on the reaction yield. As shown in Table 1, the yield of the reaction under ethanol reflux condition was higher and the reaction time was shorter than with the other solvents and solvent-free condition (entry 7). Increasing the reaction time did not increase the yield significantly (entry 8). The model reaction was carried out in the presence of silica-supported Preyssler HPA (SiO_2-PRS) and Preyssler HPA. The yield of the reaction after the same time and condition was lower than when we used NFS-PRS as a catalyst (entries 8 and 9). We believe that when we used Preyssler HPA in the supported form, due to the adsorption of the reactants on the surface of the catalyst, there was an increase in the local concentration of reactants around the active sites of the NFS-PRS which promoted the reaction effectively. This reaction was also carried out in presence of other HPAs with Keggin structures. These HPAs were not efficient for this reaction and the yields of the reaction were very low (entries 10–12).

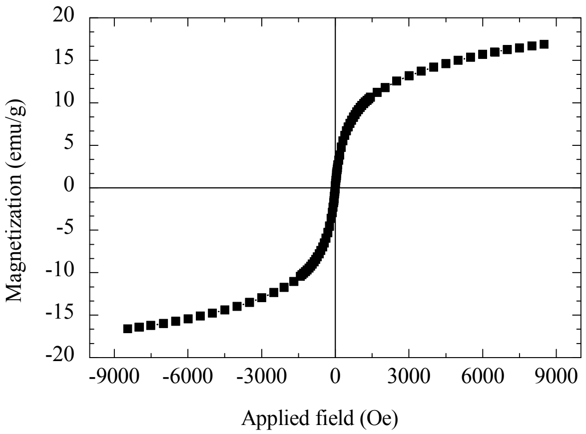

Fig. 6. VSM curve of $NiFe_2O_4$ at room temperature.

Next, to determine the optimum quantity of NFS-PRS, the reaction of terephthalic aldehyde, urea and ethyl acetoacetate was carried out under the above conditions using different amounts of catalyst (Table 2). No product was obtained in the absence of the catalyst (entry 1), indicating that the catalyst was necessary for the reaction. Increasing the amount of the catalyst increased the yield of the product **5b** (entries 2 and 3). The use of 0.02 g of catalyst resulted in the highest yield in 45 min (entry 4). Increasing the amount of the catalyst beyond this value did not increase the yield noticeably (entries 5 and 6).

Finally, after optimization of the reaction conditions, we prepared a range of bis(dihydropyrimidinone)benzene derivatives (Table 3). In all cases, 1,3-dicarbonyl compounds with

Table 2
Comparison of the amount of NFS-PRS and yield in the synthesis of bis(dihydropyrimidinone)benzene derivatives (**5b**).

Entry	Catalyst amount (g)	Time (min)	Isolated yield (%)
1	none	120	none
2	0.005	45	54
3	0.010	45	79
4	0.020	45	92
5	0.030	45	92
6	0.050	45	93

Reaction conditions: Terephthalic aldehyde **1** (1.0 mmol), urea **2** (2.5 mmol), ethyl acetoacetate **3** (2.0 mmol), EtOH/Reflux.

substituents carrying either electron-donating (entries 1–4) or electron-withdrawing (entry 5) groups reacted successfully and gave the expected products in good to excellent yields and short reaction times. Also, thiourea has no significant effect on the reaction time and yield (entries 6–8). In addition, we synthesized 3,4-dihydropyrimidin-2(1*H*)-ones and -thiones under

Table 3

Synthesis of bis(dihydropyrimidinone)benzene derivatives (**5a**–**5h**) and 3,4-dihydropyrimidin-2(1*H*)-ones and -thiones derivatives (**6a**–**6h**) using NFS-PRS as an acidic catalyst.

Entry	R_1	R_2	X	Ar	Product *	Time (min)	Isolated yield (%)	m.p. (°C)	Entry	R_1	R_2	X	Ar	Product *	Time (min)	Isolated yield (%)	m.p. (°C)
1	Me	OMe	O	—	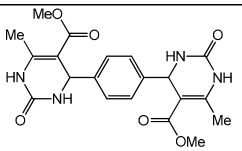 **5a**	50	94	>300 (>300 [46])	9	Me	Et	O	C_6H_5	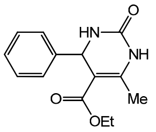 **6a**	30	93	210–211 (210–212 [48])
2	Me	OEt	O	—	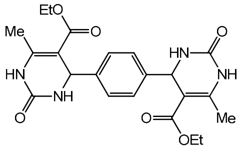 **5b**	45	92	>300 (>300 [46])	10	Me	Et	O	4-ClC_6H_4	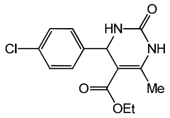 **6b**	20	94	213–214 (214–216 [48])
3	Me	Me	O	—	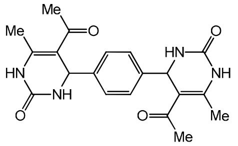 **5c**	50	93	>300 (>300 [46])	11	Me	Et	O	4-$NO_2C_6H_4$	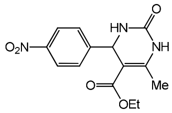 **6c**	20	92	208–210 (208–210 [48])
4	Me	Ph	O	—	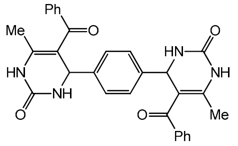 **5d**	60	90	>300 (295–298 [47])	12	Me	Et	O	4-MeC_6H_4	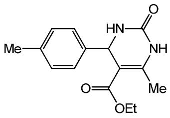 **6d**	25	93	216–218 (219–220 [48])
5	CF_3	Me	O	—	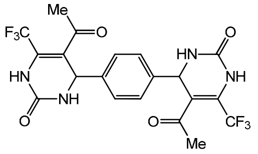 **5e**	50	94	>300 (>300 [47])	13	Me	Et	O	4-$MeOC_6H_4$	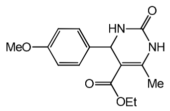 **6e**	30	90	208–210 (214–216 [48])
6	Me	Me	S	—	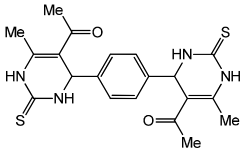 **5f**	45	95	>300 (>300 [46])	14	Me	Et	S	4-ClC_6H_4	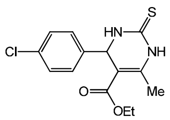 **6f**	15	95	188–190 (185–187 [48])
7	Me	OEt	S	—	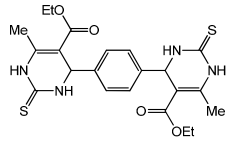 **5g**	50	93	>300 (>300 [46])	15	Me	Et	S	4-OHC_6H_4	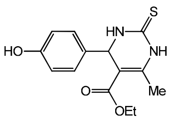 **6g**	25	93	202–203 (198–200 [48])
8	Me	OMe	S	—	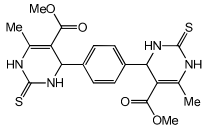 **5h**	45	92	>300 (>300 [46])	16	Me	Et	S	4-$MeOC_6H_4$	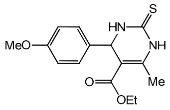 **6h**	20	92	154–156 (154–156 [48])

Reaction conditions: Terephthalic aldehyde **1** (1.0 mmol), urea and thiourea **2** (2.5 mmol), 1,3-dicarbonyl compound **3** (2.0 mmol) and NFS-PRS (0.02 g) under ethanol reflux conditions **(5a–5h)**. Aromatic aldehyde **4** (1.0 mmol), urea and thiourea **2** (1.2 mmol), 1,3-dicarbonyl compound **3** (1.0 mmol and NFS-PRS (0.02 g) under ethanol reflux conditions **(6a–6h)**.

* Selected products were identified by comparing their melting points and ^{1}H NMR, FT-IR, and MS.

Table 4
Comparison of results of NFS-PRS with other heterogeneous catalysts for the synthesis of 3,4-dihydropyrimidin-2(1*H*)-ones (**6a**).

Entry	Catalyst	Reaction conditions	Time (min)	Isolated yield (%)
1	$H_4SiW_{12}O_{40}$	AcOH/Reflux	360	80
2	$Zn(HSO_4)_2$	Solvent-free, 90 °C	150	74
3	P_2O_5–SiO_2	Solvent-free, 85 °C	120	95
4	SBSSA	Glacial HOAc, 110 °C	60	81
5	NFS-PRS	EtOH/Reflux	30	93

Reaction conditions: Benzaldehyde (1.0 mmol), urea (1.2 mmol, ethyl acetoacetate (1.0 mmol).

the optimized reaction conditions. It can be seen that by using this magnetic acidic catalyst, aromatic aldehydes containing electron-donating and electron-withdrawing groups (entries 9–16) afforded the products with good to excellent yields, and different aldehydes have no significant effect on the reaction time and yield.

To show the merit of the present catalyst, we compared the results of using NFS-PRS in the synthesis of 3,4-dihydropyrimidin-2(1*H*)-ones from benzaldehyde, urea and ethyl acetoacetate with other heterogeneous catalysts like $H_4SiW_{12}O_{40}$ heteropoly acid [49], zinc hydrogen sulfate $Zn(HSO_4)_2$ [50], P_2O_5-SiO_2 [51] and silica-bonded *S*-sulfonic acid (SBSSA) [52]. All the catalysts were tested at the same catalyst loading. As shown in Table 4, NFS-PRS (entry 5) was the most efficient catalyst and gave high yields of product in shorter reaction times. In addition, the advantages of NFS-PRS are its recyclability and very simple work-up.

A mechanism for the condensation of terephthalic aldehyde, urea and 1,3-dicarbonyl compounds in the presence of NFS-PRS for the synthesis of bis(dihydropyrimidinone)benzene is shown in Scheme 2.

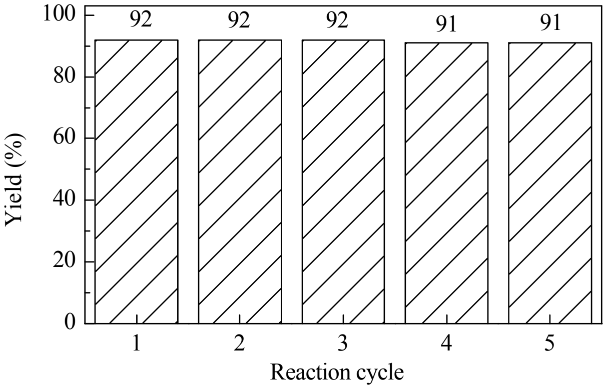

Fig. 7. Reusability of NFS-PRS for the model reaction.

From the viewpoint of green chemistry, good recovery and reusability of the catalyst are highly preferred. To show this, the same model reaction was again studied under the optimized conditions. After the completion of the reaction, NFS-PRS was separated from the reaction mixture by a magnet and thoroughly washed with methanol and chloroform to remove residual product. It was dried at 100 °C under vacuum for 2 h and reused for the reaction. As shown in Fig. 7, the catalyst can be reused at least five times without loss of activity.

The FT-IR spectra of the NFS-PRS catalyst before use (fresh) and after reuse for five times (recovered) were obtained. As shown in Fig. 8, the FT-IR spectrum of the recovered NFS-PRS

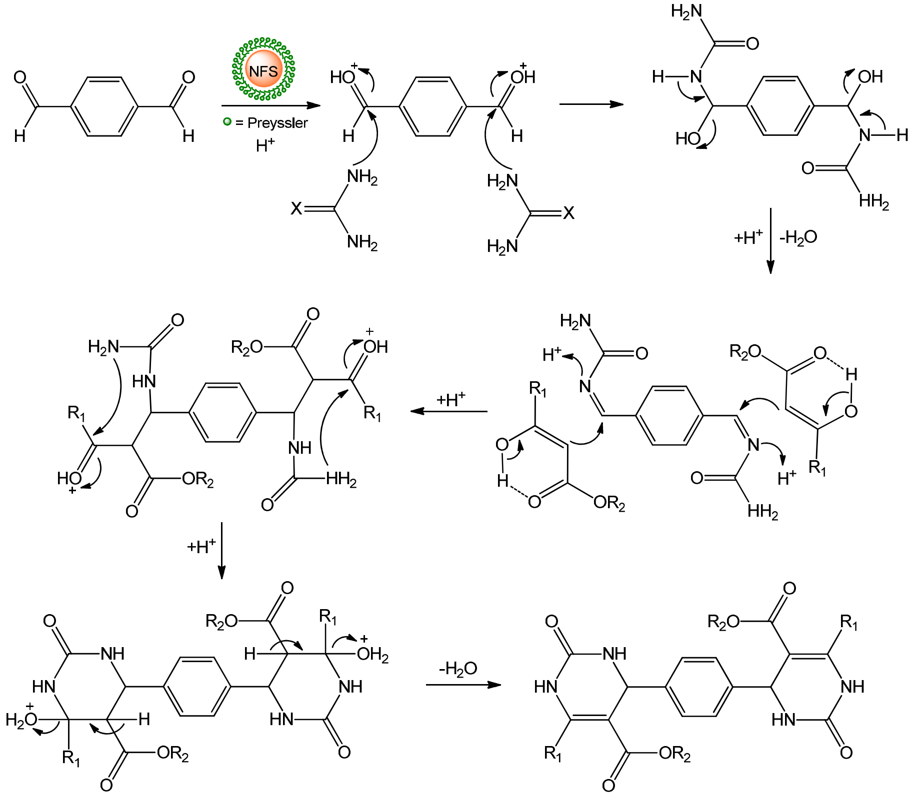

Scheme 2. Proposed mechanism for the generation of bis(dihydropyrimidinone)benzene derivatives.

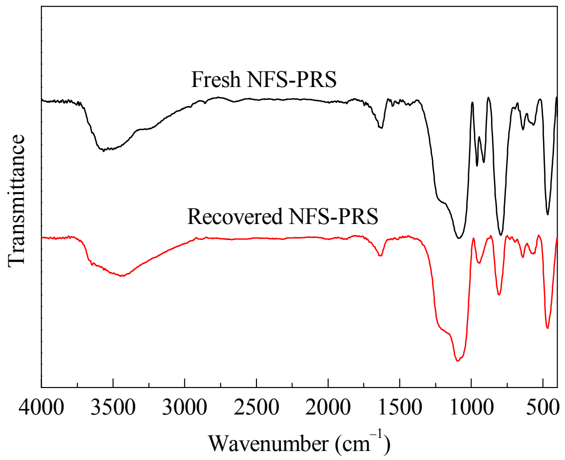

Fig. 8. FT-IR spectra of (a) fresh and (b) recovered (after five times) NFS-PRS.

showed that the structure of the catalyst remained the same after five runs. In addition, the weight of the recovered catalyst was the same as the amount of the fresh catalyst used the first time in the reaction.

4. Conclusions

We have prepared a novel magnetic catalyst containing Preyssler HPA supported on silica coated nickel ferrite NPs (NFS-PRS) for the synthesis of bis(dihydropyrimidinone)benzene and 3,4-dihydropyrimidin-2(1*H*)-ones and -thiones derivatives by the Biginelli reaction. The Preyssler HPA provided adequate acidic sites to give the excellent catalytic activity of NFS-PRS. This magnetic catalyst can be easily removed from the reaction mixture by an external magnet, and it was reused several times without loss of catalytic activity. In addition to the synthesis of these products by the Biginelli reaction, the environmentally benign NFS-PRS catalyst is potentially promising for other acid-catalyzed chemical reactions.

Acknowledgments

The authors are thankful to Ferdowsi and Islamic Azad University, Mashhad and Bandar Abbas Branches for financial support.

References

[1] Saiyed Z M, Telang S D, Ramchand C N. *BioMagn Res Technol*, 2003, 1: 2
[2] Sahoo S K, Labhasetwar V. *Drug Discovery Today*, 2003, 8: 1112
[3] Polshettiwar V, Luque R, Fihri A, Zhu H, Bouhrara M, Basset J M. *Chem Rev*, 2011, 111: 3036
[4] Li P H, Wang L, Zhang L, Wang G W. *Adv Synth Catal*, 2012, 354: 1307
[5] Wittmann S, Schätz A, Grass R N, Stark W J, Reiser O. *Angew Chem Int Ed*, 2010, 49: 1867
[6] Kaboudin B, Mostafalu R, Yokomatsu T. *Green Chem*, 2013, 15: 2266
[7] Wang Y H, Lee J K. *J Mol Catal A*, 2007, 263: 163
[8] Rossi L M, Silva F P, Vono L L R, Kiyohara P K, Duarte E L, Itri R,

Graphical Abstract

Chin. J. Catal., 2015, 36: 299–307 doi: 10.1016/S1872-2067(14)60265-5

Preyssler heteropolyacid supported on silica coated NiFe$_2$O$_4$ nanoparticles for the catalytic synthesis of bis(dihydropyrimidinone)benzene and 3,4-dihydropyrimidin-2(1*H*)-ones

Hossein Eshghi, Ali Javid *, Amir Khojastehnezhad *, Farid Moeinpour, Fatemeh F. Bamoharram, Mehdi Bakavoli, Masoud Mirzaei
Ferdowsi University of Mashhad, Iran; Islamic Azad University, Iran

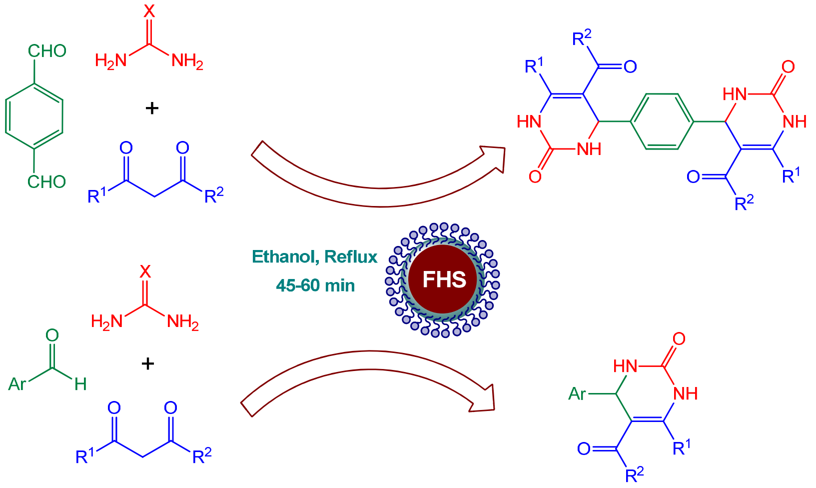

A novel magnetic acidic catalyst comprising Preyssler HPA supported on silica coated nickel ferrite nanoparticles was prepared and its catalytic activity in the Biginelli reaction was investigated.

Landers R, Machado G. *Green Chem*, 2007, 9: 379

[9] Yi D K, Lee S S, Ying J Y. *Chem Mater*, 2006, 18: 2459

[10] Polshettiwar V, Varma R S. *Org Biomol Chem*, 2009, 7: 37

[11] Aschwanden L, Panella B, Rossbach P, Keller B, Baiker A. *ChemCatChem*, 2009, 1: 111

[12] Oliveira R L, Kiyohara P K, Rossi L M. *Green Chem*, 2010, 12: 144

[13] Karimi B, Farhangi E. *Chem Eur J*, 2011, 17: 6056

[14] Schätz A, Grass R N, Stark W J, Reiser O. *Chem Eur J*, 2008, 14: 8262

[15] Tucker-Schwartz A K, Garrell R L. *Chem Eur J*, 2010, 16: 12718

[16] Karimi B, Farhangi E. *Adv Synth Catal,* 2013, 355: 508

[17] Rostamnia S, Lamei K, Mohammadquli M, Sheykhan M, Heydari A. *Tetrahedron Lett*, 2012, 53: 5257

[18] Sheykhan M, Mohammadnejad H, Akbari J, Heydari A. *Tetrahedron Lett*, 2012, 53: 2959

[19] Mamani L, Heydari A, Sheykhan M. *Appl Catal A*, 2010, 384: 122

[20] Wang S G, Zhang Z H, Liu B, Li J L. *Catal Sci Technol*, 2013, 3: 2104

[21] Rafiee E, Eavani S. *Green Chem*, 2011, 13: 2116

[22] Rafiee E, Eavani S. *J Mol Catal A*, 2013, 373: 30

[23] Rafiee E, Eavani S, Khodayari M. *Chin J Catal*, 2013, 34: 1513

[24] Chaudhuri A, Mandal M, Mandal K. *J Alloys Compd*, 2009, 487: 698

[25] Köseoğlu Y, Baykal A, Toprak M S, Gözüak F, Başaran A C, Aktaş B. *J Alloys Compd*, 2008, 462: 209

[26] Hou X Y, Feng J, Xu X D, Zhang M L. *J Alloys Compd*, 2010, 491: 258

[27] Goldman A. Modern Ferrite Technology. New York: Van Nostrand Reinhold, 1990

[28] Hekmatshoar R, Sadjadi S, Shiri S, Heravi M M, Beheshtiha Y S. *Synth Commun*, 2009, 39: 2549

[29] Hafizi A, Ahmadpour A, Heravi M M, Bamoharram F F. *Pet Sci Technol*, 2014, 32: 1022

[30] Wu S S, Liu P, Leng Y, Wang J. *Catal Lett*, 2009, 132: 500

[31] Javid A, Khojastehnezhad A, Heravi M M, Bamoharram F F. *Syn React Inorg Met Org*, 2012, 42: 14

[32] Hafizi A, Ahmadpour A, Heravi M M, Bamoharram F F, Khosroshahi M. *Chin J Catal*, 2012, 33: 494

[33] Bamoharram F F, Heravi M M, Ebrahimi J, Ahmadpour A, Zebarjad M. *Chin J Catal*, 2011, 32: 782

[34] Madhusudhan Rao P, Wolfson A, Kababya S, Vega S, Landau M V. *J Catal*, 2005, 232: 210

[35] Ghiaci M, Zarghani M, Khojastehnezhad A, Moeinpour F. *RSC Adv*, 2014, 4: 15496

[36] Ghiaci M, Zarghani M, Moeinpour F, Khojastehnezhad A. *Appl Organomet Chem*, 2014, 28: 589

[37] Davoodnia A, Khojastehnezhad A, Tavakoli-Hoseini N. *Bull Korean Chem Soc*, 2011, 32: 2243

[38] Khojastehnezhad A, Moeinpour F, Davoodnia A. *Chin Chem Lett*, 2011, 22: 807

[39] Khojastehnezhad A, Rahimizadeh M, Eshghi H, Moeinpour F, Bakavoli M. *Chin J Catal*, 2014, 35: 376

[40] Eshghi H, Khojastehnezhad A, Moeinpour F, Bakavoli M, Seyadi S M, Abbasi M. *RSC Adv*, 2014, 4: 39782

[41] Khojastehnezhad A, Rahimizadeh M, Moeinpour F, Eshghi H, Bakavoli M. *Compt R C*, 2014, 17: 459

[42] Gharib A, Jahangir M, Scheeren J W. *Polish J Chem Technol*, 2011, 13(2): 11

[43] Hamadi H, Kootia M, Afshari M, Ghiasifar Z, Adibpour N. *J Mol Catal A*, 2013, 373: 25

[44] Vivekanandhan S, Venkateswarlu M, Carnahan D, Misra M, Mohanty A K, Satyanarayana N. *Ceramics Int*, 2013, 39: 4105

[45] Wang H X, Zhang W, Zhang F L, Cao Y, Su W H. *J Magn Magn Mater*, 2008, 320: 1916

[46] Tu S J, Zhu X T, Fang F, Zhang X J, Zhu S L, Li T J, Shi D Q, Wang X S, Ji S J. *Chin J Chem*, 2005, 23: 596

[47] Azizian J, Mohammadi M K, Firuzi O, Mirza B, Miri R. *Chem Biol Drug Des*, 2010, 75: 375

[48] Zeinali-Dastmalbaf M, Davoodnia A, Heravi M M, Tavakoli-Hoseini N, Khojastehnezhad A, Zamani H A. *Bull Korean Chem Soc*, 2011, 32: 656

[49] Niknam Kh, Daneshvar N. *Heterocycles*, 2007, 71: 373

[50] Niknam Kh, Ali Zolfigol M, Hossieninejad Z, Daneshvar N. *Chin J Catal*, 2007, 28: 591

[51] Hasaninejad A, Zare A, Jafari F, Moosavi-Zare A R. *E-J Chem*, 2009, 6: 459

[52] Tajbakhsh M, Ranjbar Y, Masuodi A, Khaksar S. *Chin J Catal*, 2012, 33: 1542